Interaction between Poly(ethylene glycol) and $C_{12}E_8$ Investigated by Dynamic Light Scattering, Time-Resolved Fluorescence Quenching, and Calorimetry

E. Feitosa,*,† W. Brown,‡ K. Wang,‡ and P. C. A. Barreleiro§

Departamento de Física, IBILCE/UNESP, 15055-000, São José do Rio Preto, SP, Brazil; Department of Physical Chemistry, University of Uppsala, Box 532, 751 21, Sweden; and Physical Chemistry 1, Center for Chemistry and Chemical Engineering, University of Lund, P.O. Box 124, S-221 00 Lund, Sweden

Received April 23, 2001; Revised Manuscript Received September 25, 2001

ABSTRACT: Dynamic light scattering (DLS), time-resolved fluorescence quenching (TRFQ), and isothermal titration microcalorimetry have been used to show that, in dilute solution, low molecular weight poly(ethylene glycol) (PEG, $M_w = 12$ kDa) interacts with the nonionic surfactant octaethylene glycol *n*-dodecyl monoether, $C_{12}E_8$, to form a complex. Whereas the relaxation time distributions for the binary $C_{12}E_8$/water and PEG/water systems are unimodal, in the ternary mixtures they may be either uni- or bimodal depending on the relative concentrations of the components. At low concentrations of PEG or surfactant, the components of the relaxation time distribution are unresolvable, but the distribution becomes bimodal at higher concentrations of either polymer or surfactant. For the ternary system in excess surfactant, we ascribe, on the basis of the changes in apparent hydrodynamic radii and the scattered intensities, the fast mode to a single micelle, the surface of which is associated with the polymer and the slow mode to a similar complex but containing two or three micelles per PEG chain. Titration microcalorimetry results show that the interaction between $C_{12}E_8$ and PEG is exothermic and about 1 kJ mol^{-1} at concentrations higher than the cmc of $C_{12}E_8$. The aggregation number, obtained by TRFQ, is roughly constant when either the PEG or the $C_{12}E_8$ concentration is increased at a given concentration of the second component, owing to the increasing amount of surfactant micelles inside the complex.

Introduction

There is considerable interest in colloidal systems consisting of mixtures of polymers and surfactants in solution.[1−13] As a consequence of their mutual interactions, the polymer may increase the solubility of a surfactant, which in turn will influence the adsorption characteristics of the polymer.[2] The different properties of the mixtures are attributed to the complexation of the polymer with the surfactant. Polymer−surfactant complexes are colloidal structures with properties differing from those of the pure components; stability and solubility are the properties usually improved by mixing polymers and surfactants.[3,4,7]

The affinity of a surfactant for a polymer depends on the physical properties of the components (hydrophobicity, molar mass, electrostatic nature, etc.) as well as on the surrounding medium (temperature, ionic strength or pH, solvent polarity, etc.). Complex formation between polymers and surfactants has been studied using a number of techniques, for example, viscometry,[6] tensiometry,[7] calorimetry,[11] fluorometry,[13] and light scattering.[8−10,12]

The complexity and variety of ternary polymer/surfactant/solvent systems compared to the corresponding binary systems are the main reasons for the absence of a general theory or model for polymer/surfactant complexation, which is a highly system-dependent phenomenon. It has been observed, for example, that anionic surfactants have a higher affinity for neutral polymers than cationic surfactants, which, in turn, interact much more strongly than nonionic surfactants with neutral polymers. The nature of the surfactant headgroup as well as the structure and size of the micelles formed are important factors determining the interaction pattern. As an example, SDS has a stronger affinity for the neutral polymer poly(ethylene oxide) (PEO) than CTAB despite their similar micellar sizes and degrees of counterion dissociation;[3] $C_{12}E_5$, on the other hand, which forms larger micelles than $C_{12}E_8$, has a much higher affinity for PEO at a given temperature below the clouding temperature of $C_{12}E_5$.[8−10]

Ternary systems consisting of neutral polymers and nonionic surfactants in aqueous solution have been described as noninteracting[6] or very weakly interacting only when the polymer has a higher hydrophobicity.[7,11] Earlier, however, we have shown by light scattering that high molar mass (6.0×10^5 Da) PEO forms complexes with both $C_{12}E_5$[8,9] and $C_{12}E_8$[10] although the cmc's of these surfactants are not significantly changed in the presence of the PEO, and the aggregation number may be equal to, smaller than, or larger than that of the polymer-free micelles depending on the system and on the concentration ranges investigated.[8−10] The formation of micellar clusters within the polymer coil was associated with the excluded volume effect of the polymer.[8] These results prompted us to look at the influence of a low molar mass PEG ($M_w = 12$ kDa) on the interaction with the nonionic surfactant $C_{12}E_8$. The techniques used were dynamic light scattering, time-resolved fluorescence quenching, and titration calorimetry.

† IBILCE/UNESP.
‡ University of Uppsala.
§ University of Lund.
* To whom correspondence should be addressed: phone +55 17 221 22 38; Telefax +55 17 221 22 47; e-mail eloi@df.ibilce.unesp.br.

10.1021/ma010696w CCC: $22.00
Published on Web 12/04/2001

Experimental Section

Materials. Octaethylene glycol *n*-dodecyl monoether, $C_{12}E_8$, and poly(ethylene glycol), PEG, $M_w = 12$ kDa, were used as received respectively from Nikko Chemicals, Japan, and Fluka. Pyrene and 3,4-dimethylbenzophenone (99%, DMBP), from Aldrich, were recrystallized from ethanol.

Dynamic Light Scattering (DLS). Measurements were made with the same apparatus described previously.[8−10,12] A 488 nm Ar ion laser was used as light source, and a detector system was an ITT FW 130 photomultiplier connected to an ALV-Langen Co. multibit, multitau autocorrelator and a microcomputer through a digitalized amplifier/discriminator system.

The inverse Laplace transform (ILT) analysis of the normalized intensity autocorrelation functions, $g_2(t)$, was performed using the algorithm REPES[14] to obtain the unknown relaxation time distribution, $\tau A(\tau)$, according to eq 1

$$g^1(t) = \int_{-\infty}^{+\infty} \tau A(\tau) e^{-t/\tau} \, d \ln \tau \qquad (1)$$

where $g_1(t)$ accounts for the electric field autocorrelation function, $g_2(t) - 1 = \beta |g_1(t)(t)|^2$, β is a nonideality factor (<1) which depends on the experimental geometry, and τ is the relaxation time. The relaxation time distribution is expressed as a $\tau A(\tau)$ vs log τ profile, with $\tau A(\tau)$ in arbitrary units to provide an equal area representation.[15] For broad distributions of the relaxation time the unsmoothed analysis yields multiple peaks, and the diffusion coefficient for each mode is calculated from the moments of the distribution, according to the relation $D = \Gamma/q^2$, in the limit of zero scattering angle (θ), where $q = (4\pi n_0/\lambda) \sin(\theta/2)$ is the scattering vector, λ is the wavelength, n_0 is the solvent refractive index, and $\Gamma = 1/\tau$ is the relaxation rate.

The hydrodynamic radius (R_H) was obtained from the diffusion coefficient at infinite dilution (D_0) and using the Stokes−Einstein relation (eq 2)

$$R_H = kT/\pi\eta_0 D_0 \qquad (2)$$

where k is the Boltzmann constant, T is the absolute temperature, and η_0 is the solvent viscosity.

The scattering measurements were made at different concentrations of either surfactant or polymer, holding constant the concentration of the other component, and also at selected ratios of surfactant to polymer.

Time-Resolved Fluorescence Quenching (TRFQ). Time-resolved fluorescence decay data were collected with the single photon counting technique. The setup uses a mode-locked Nd:YAG laser to synchronously pump a cavity-dumped dye laser for the excitation, using the dye DCM and frequency doubling in a KDP crystal. The excitation wavelength was 320 nm, and the pyrene monomer emission was measured at 395 nm. The single photon count rate was kept low enough to prevent two-photon excitation. The detailed description of the method and equipment are given elsewhere.[15] All measurements were performed at 20 °C in equilibrium with air using pyrene and 3,4-dimethylbenzophenone (DMBP) as probe and quencher, respectively. In the case of stationary probe and quencher and Poisson distribution of the quencher, the decay curves were fitted to the simple Infelta−Tachiya model[17]

$$F(t) = F(0) \exp[-t/\tau_0 + \langle n \rangle \{\exp(-k_q t) - 1\}] \qquad (3)$$

where $F(t)$ describes the time evolution of the fluorescence intensity, $F(0)$ is the fluorescence intensity at time zero, τ_0 is the natural lifetime of pyrene obtained from separate experiments without quencher, $\langle n \rangle$ is the average number of quenchers in a micelle, and k_q is the first-order quenching rate constant.

The surfactant aggregation number, N_{agg}, was calculated from (eq 4)

$$N_{agg} = \langle n \rangle [S_m]/[Q_m] \qquad (4)$$

where $[S_m]$ and $[Q_m]$ are, respectively, the surfactant and quencher concentration within the micelles. The quencher has a low solubility in water and preferentially solubilizes into the hydrophobic environment provided by the micelle. Since the free concentrations of surfactant and quencher are negligible, $[S_m]$ and $[Q_m]$ may be replaced by the total concentration of surfactant and quencher, respectively.

Isothermal Titration Microcalorimetry. The heat of reaction between $C_{12}E_8$ and PEG was measured in a stainless steel titration vessel of 3 mL in the prototype of the TAM (thermal activity monitor) four-channel microcalorimetric at 25 °C. The calorimetric signal was calibrated electrically, using insertion heaters immersed in water inside the vessel and by dissolution of propanol in water.[18] In the experimental procedure small aliquots of the $C_{12}E_8$ micellar solution (or PEG solution) were added to water or polymeric solution (or $C_{12}E_8$ micellar solution) in the calorimeter vessel. The additions were made using a gastight Hamilton syringe connected with a computer-operated syringe drive to control the injection volume, and the rate could be controlled with great precision. The uptake/release of heat (enthalpy) is measured for each injection by integration of the area under the calorimetric trace.

Results and Discussion

1. Dynamic Light Scattering (DLS). 1.1. Binary $C_{12}E_8$/Water and PEG/Water Systems. Figure 1a shows typical intensity correlation functions and relaxation time distributions for the binary systems of $C_{12}E_8$ and low molar mass PEG ($M_w = 12$ kDa) in water. These diagrams show that binary aqueous solutions of both $C_{12}E_8$ and PEG at 20 °C are close to monodisperse, being characterized by sharp unimodal relaxation time distributions up to 5.0 wt % of PEG and 10 wt % of $C_{12}E_8$. The concentration dependence of the translational diffusion coefficient is positive for binary solutions of $C_{12}E_8$ micelles and PEG (Figure 1b). At 20 °C PEG coil and $C_{12}E_8$ micelles have approximately the same mean hydrodynamic radius, $R_H \sim 3.2$ nm, obtained from the diffusion coefficient values at infinite dilution using the Stokes−Einstein relation (eq 2).

1.2. Ternary PEG/$C_{12}E_8$/Water System. (*a) Constant PEG and Varying $C_{12}E_8$ Concentration.* The relaxation time distribution for the ternary PEG/$C_{12}E_8$/water system may be either uni- or bimodal depending on the concentration of the two components. Figure 1a shows the autocorrelation function and the corresponding bimodal relaxation time distribution for PEG 5.0 wt % mixed with $C_{12}E_8$ 10 wt %. The linear dependence of Γ on the squared scattering vector (q^2) with the fitting curve passing through the origin (results not shown) demonstrates diffusive processes for both the fast and slow modes of the distribution.

Figure 2 shows the relaxation time distributions for three fixed concentrations of PEG (1.0, 3.0, and 5.0 wt %) and increasing up to 10 wt % $C_{12}E_8$ concentration. At 1.0 wt % PEG the distribution is unimodal, but the peak broadens progressively up to about 4 wt % $C_{12}E_8$. When the surfactant concentration is increased above this value, the distribution splits into two well-separated and well-defined components. The fast mode we attribute to a single surfactant micelle complexed with a PEG chain and the slower mode to similar complexes containing more than one micelle of $C_{12}E_8$. As the PEG concentration is raised, the multimicellar complex is preferred at a progressively lower $C_{12}E_8$ concentration.

Translational diffusion coefficients are shown as a function of $C_{12}E_8$ concentration in Figure 3 at fixed PEG concentrations. The plots for the fast mode exhibit

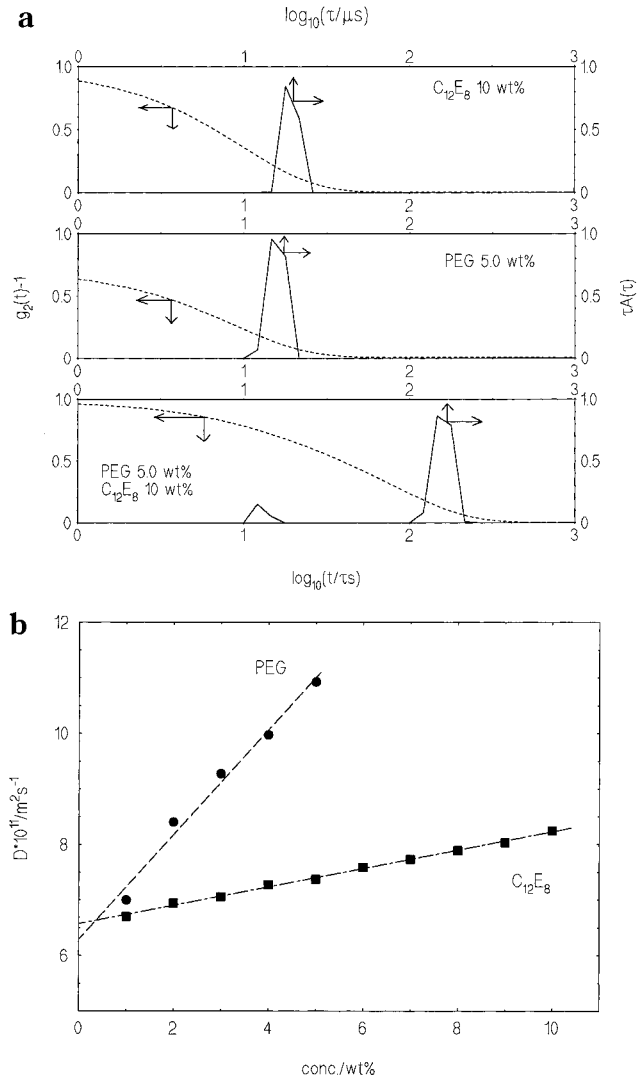

Figure 1. (a) Normalized intensity autocorrelation functions, $g_2(t) - 1$, and relaxation time distribution for the binary $C_{12}E_8$ 10 wt % and PEG 5.0 wt % in water and the ternary PEG/$C_{12}E_8$/water, 5.0 wt % PEG and 10 wt % $C_{12}E_8$. (b) Translational diffusion coefficients of PEG coils and PEG-free micelles as a function of concentration. Measurements at 20 °C and $\theta = 90°$.

positive concentration dependence as is the case for the binary aqueous systems of micelle or PEG. We include for comparison a plot for 1.0 wt % PEG which exhibits no splitting. From the intercepts the apparent hydrodynamic radii were estimated using eq 2, and these values are plotted in Figure 4 as a function of PEG concentration for the fast and slow modes. The relative amplitudes of the slow to the fast modes are shown in Figure 5. Figure 6 shows the gradual change in the corresponding absolute scattered intensity with PEG or $C_{12}E_8$ concentration up to 4.0 or 15 wt %, respectively. For the slow mode, R_H decreases slightly up to ca. 1.0 wt % PEG, while above this concentration it increases with PEG concentration, suggesting the formation of larger multimicellar complexes. At a given concentration of PEG the A_S/A_F ratio increases with $C_{12}E_8$ concentration, showing that the PEG−$C_{12}E_8$ complexes contribute more to the total scattered intensity than free micelles at the corresponding concentration; see also Figure 6b for the dependence of the scattered intensity on the concentration of polymer.

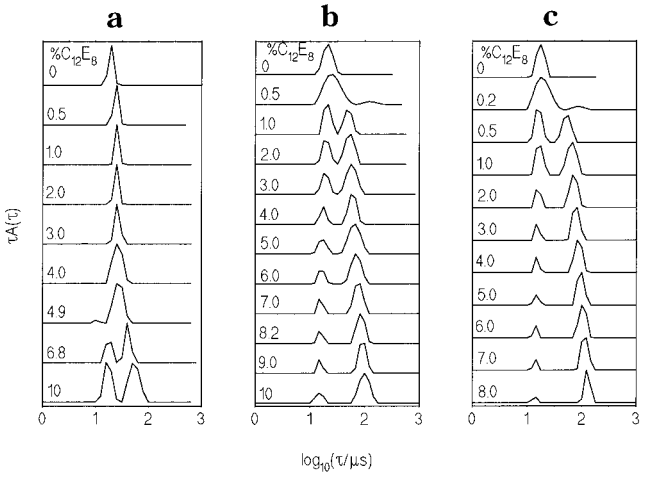

Figure 2. Relaxation time distributions for the ternary PEG/$C_{12}E_8$/water system at (a) 1.0, (b) 3.0, and (c) 5.0 wt % PEG and increasing concentration of $C_{12}E_8$, as shown. Measurements at 20 °C.

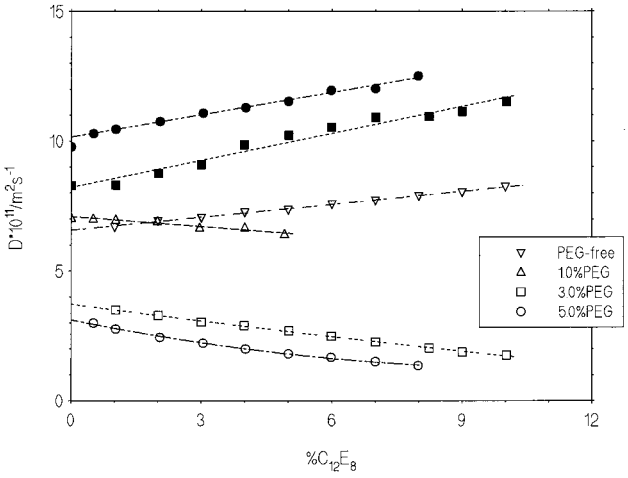

Figure 3. Fast and slow mode diffusion coefficients for the ternary PEG/$C_{12}E_8$/water system as a function of $C_{12}E_8$ concentration at selected PEG concentrations, as shown.

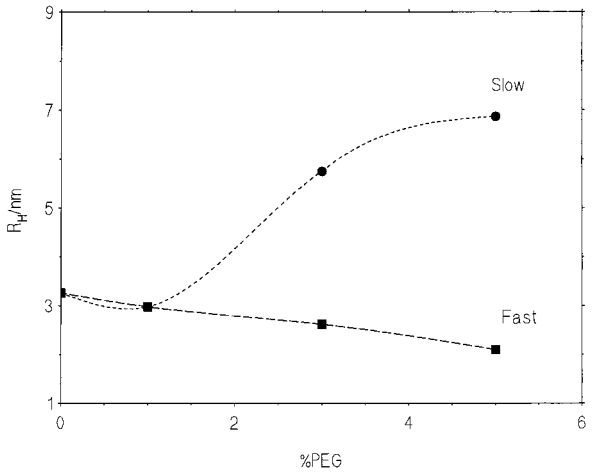

Figure 4. Hydrodynamic radii for the fast (■) and slow (●) modes obtained at infinite dilution of $C_{12}E_8$ as a function of polymer concentration.

(b) Constant Surfactant and Varying PEG Concentration. Figure 7 shows relaxation time distributions for the ternary PEG/$C_{12}E_8$/water system at fixed surfactant concentrations of 5, 10, and 15 wt % and increasing PEG

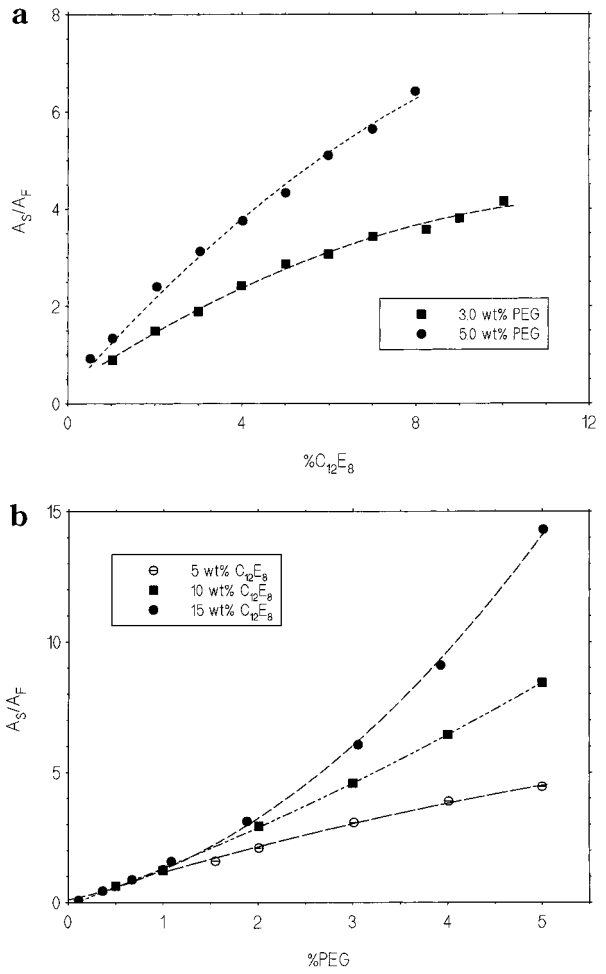

Figure 5. Dependence of the slow to the fast mode relative amplitudes, A_S/A_F, for the ternary system on $C_{12}E_8$ (a) and PEG (b) concentration at selected PEG or $C_{12}E_8$ concentrations, as shown.

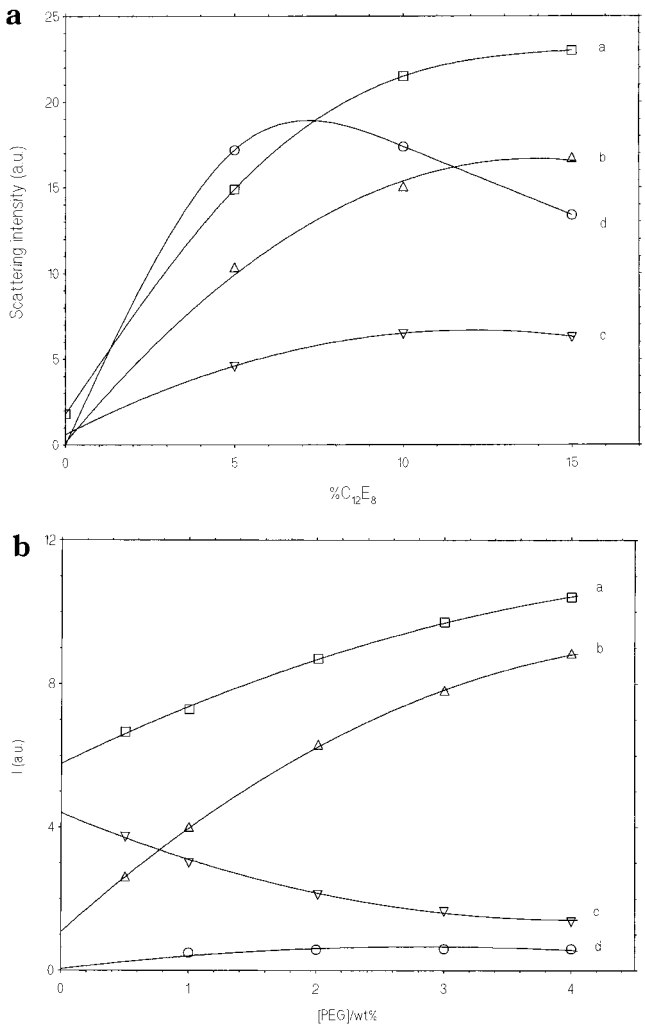

Figure 6. Scattering intensities (a) as a function of $C_{12}E_8$ concentration in the presence and absence of PEG 2.0 wt % and (b) as a function of PEG concentration in the absence and presence of 10 wt % $C_{12}E_8$. Letters *a*, *b*, *c*, and *d* indicate the total scattered intensity and the slow mode, fast mode, and pure PEG or $C_{12}E_8$ scattered intensity, respectively.

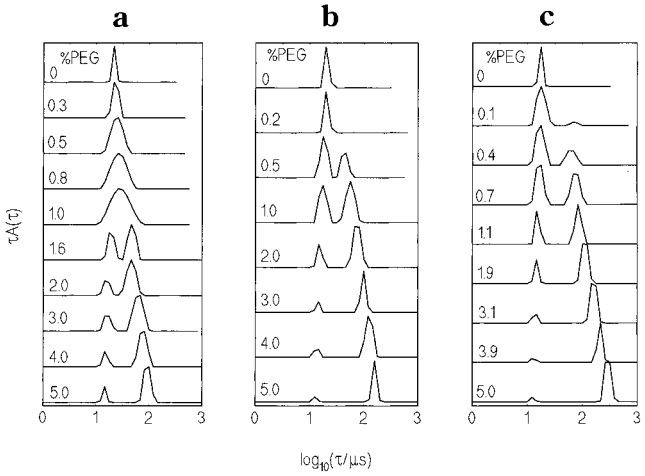

Figure 7. Relaxation time distributions for the ternary PEG/$C_{12}E_8$/water system at (a) 5, (b) 10, and (c) 15 wt % $C_{12}E_8$ and increasing concentration of PEG, as shown.

concentration. At the lowest concentrations of PEG or $C_{12}E_8$, the distributions are unimodal, becoming bimodal at higher concentrations of both components.

The effect of PEG concentration on the fast and slow mode diffusion coefficients is shown in Figure 8. There is a positive, nonlinear PEG concentration dependence for the fast mode and a negative nonlinear dependence for the slow mode. Extrapolation to zero PEG concentration yields approximate values for the apparent hydrodynamic radii using eq 2. The latter are shown in Figure 9 as a function of the surfactant concentration. For both the fast and slow modes the effect of $C_{12}E_8$ concentration on R_H resembles that shown in Figure 4 for the effect of PEG on R_H, meaning that, like PEG, the addition of $C_{12}E_8$ favors the stability of the multimicellar complexes. The increasing importance of the slow mode when either the added surfactant or PEG concentration is increased is shown in Figure 5.

By comparison with the data for the binary systems, the results for the ternary systems suggest that the fast mode at higher concentrations of $C_{12}E_8$ is not identical with free $C_{12}E_8$ micelles as was the case in the ternary mixtures of high molar mass PEO ($M_w = 600$ kDa) with the surfactants $C_{12}E_5$ and $C_{12}E_8$ reported previously.[8−10] For both the fast and slow modes, R_H at infinite PEG dilution and at low concentrations of $C_{12}E_8$ is of similar size to the isolated PEG coil, but at higher concentrations of the surfactant, however, R_H is smaller (larger) for the fast (slow) mode (Figure 9). Thus, we conclude that the fast mode does not correspond to the diffusion

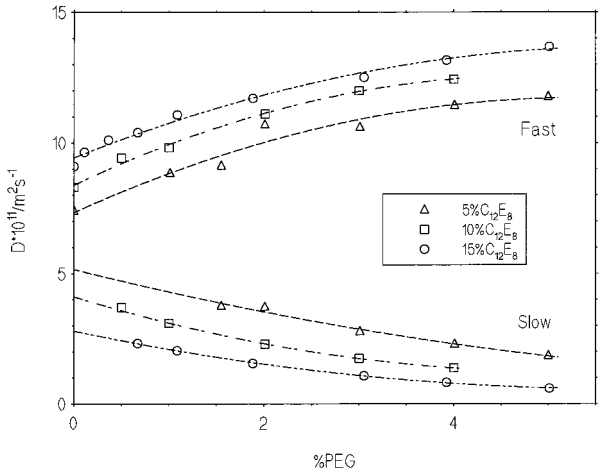

Figure 8. Effect of PEG concentration on the fast and slow mode diffusion coefficient for the ternary PEG/$C_{12}E_8$/water system at selected concentrations of $C_{12}E_8$.

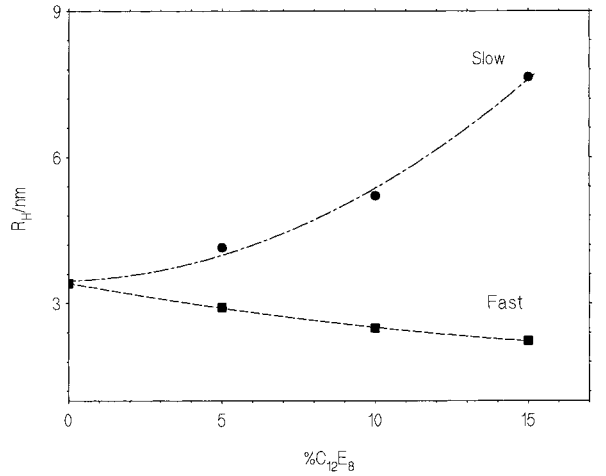

Figure 9. Hydrodynamic radii for the fast (■) and slow (●) modes obtained at infinite dilution of PEG as a function of $C_{12}E_8$ concentration.

of a single PEG chain since the fast mode scattering intensity is greater than that of pure PEG but is lower than that of pure $C_{12}E_8$ micelles (Figure 6); i.e., the fast mode does not correspond to either $C_{12}E_8$ micelles or PEG coils. Instead, we infer that it corresponds to small PEG−$C_{12}E_8$ complexes. This situation is supported by Figure 6a, showing scattered intensity data for the system containing PEG (2.0 wt %) to which $C_{12}E_8$ is progressively added and comparing these with the intensities for binary $C_{12}E_8$ solutions of the same concentration range. Figure 7b shows the analogous plot for the system containing 10 wt % $C_{12}E_8$, to which PEG is progressively added.

We thus interpret the fast mode of the bimodal distribution as deriving from a single $C_{12}E_8$ micelle complexed with a single PEG chain, i.e., a single micelle with a single PEG chain wrapped around it. As the concentration of PEG (or $C_{12}E_8$) is increased, the fast mode complex apparently becomes smaller (Figure 9), although one cannot unambiguously distinguish between changes in size and changes in interactions when the measurements are made at finite concentrations. The slow mode hydrodynamic radius and intensity, on the other hand, increase with PEG concentration (Figure 9). One possible interpretation in this case is that several micelles are associated with the same chain.

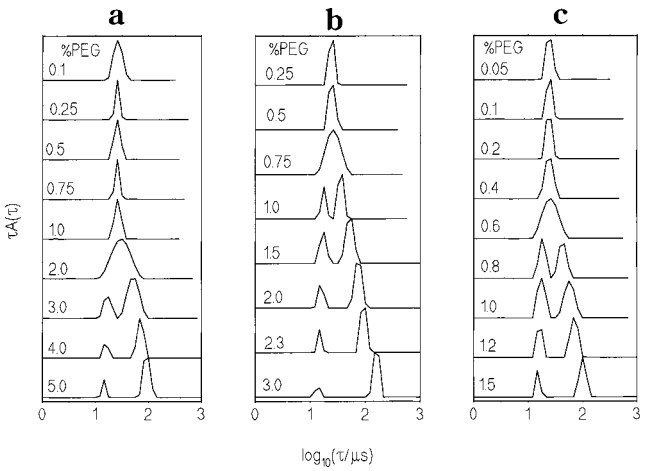

Figure 10. Relaxation time distributions for the ternary PEG/$C_{12}E_8$/water system at different $C_{12}E_8$/PEG ratios (a) 1.0, (b) 5.0, and (c) 10 with increasing concentration of PEG, as shown.

A 12 kDa PEG has about 273 CH_2-CH_2-O monomers, giving a PEG chain contour length of about 49 nm (monomer length about 0.18 nm). The circumference of a free $C_{12}E_8$ micelle is about 18 nm, so that a PEG chain of this length is able to wrap effectively about the surface of a $C_{12}E_8$ micelle. At low surfactant concentrations the smaller complex (single micelle complex) dominates the distribution, while the interaction of several micelles with one chain will be favored by larger amounts of either the polymer or surfactant. The surfactant concentration at which the multimicelle complex first appears is lowered as the concentration of PEG is increased (about 5.0, 0.7, and 0.3 wt % respectively for 1.0, 3.0, and 5.0 wt % PEG) probably owing to excluded-volume effects.

(c) Constant $C_{12}E_8$/PEG Ratio and Varying Total Concentration. Figure 10 shows relaxation time distributions for the ternary PEG/$C_{12}E_8$/water system (20 °C) at selected $C_{12}E_8$/PEG ratios. The results are rather similar to those discussed above for fixed $C_{12}E_8$ or PEG concentrations and varying the concentration of the other component. At low concentrations of PEG and/or $C_{12}E_8$, the distribution is single modal but becomes bimodal at higher concentration ratios. The higher the $C_{12}E_8$/PEG ratio, the lower (higher) the PEG ($C_{12}E_8$) concentration at which the distribution becomes bimodal, with the splitting occurring at a roughly constant total concentration of about 7−8 wt %. Figure 11a illustrates the behavior of the diffusion coefficients at ratios 1, 5, and 10 on the PEG concentration. Figure 11b shows R_H for the fast and slow modes obtained at infinite dilution. Again, we observe an apparently smaller size as the ratio increases, suggesting that at low concentrations of the components a smaller single micelle complex is favored. A possible interpretation of the slow mode observed in the DLS data is that segregation of the components occurs at higher concentrations of PEG or $C_{12}E_8$, with formation of large PEG and/or $C_{12}E_8$ clusters. Time-resolved fluorescence and calorimetry experiments were made to explore this alternative.

2. Time-Resolved Fluorescence Quenching (TRFQ). According to our TRFQ results (not shown here), the addition of PEG to the surfactant solution (5.0 wt % $C_{12}E_8$) does not modify the pyrene fluorescence

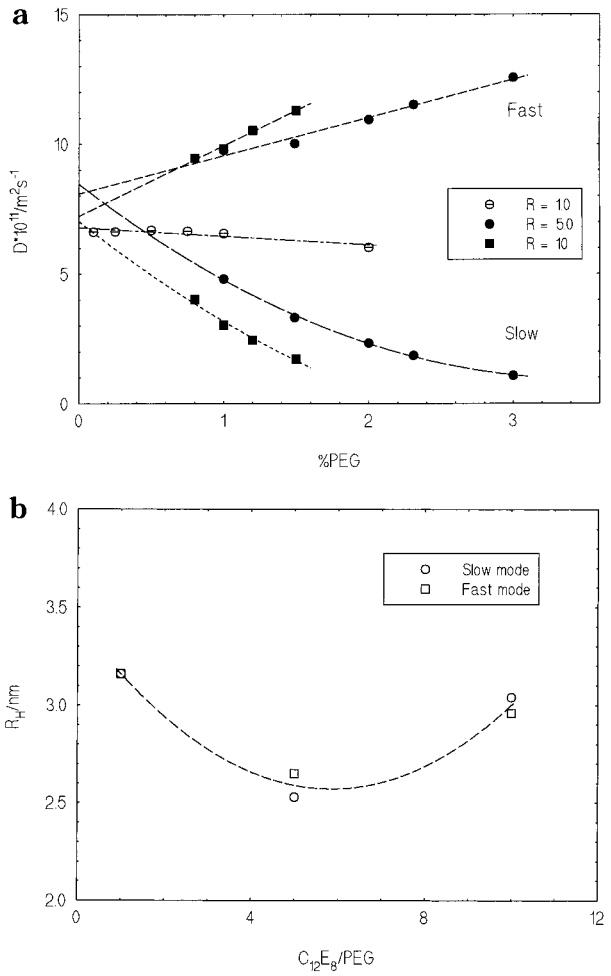

Figure 11. (a) Fast and slow mode diffusion coefficients for the ternary PEG/$C_{12}E_8$/water system as a function of PEG concentration at $C_{12}E_8$/PEG ratio = 1, 5 and 10. (b) Hydrodynamic radius of the PEG−$C_{12}E_8$ complex for the fast mode function of $C_{12}E_8$/PEG concentration ratio.

lifetime $\tau_0 \sim 197$ ns. Up to ca. 5 wt % $C_{12}E_8$, τ_0 depends on the surfactant concentration, and the addition of PEG decreases τ_0 only slightly (by ca. 5 ns). Within the experimental error, PEG does not affect N_{agg}; up to about 5 wt % PEG or $C_{12}E_8$ N_{agg} of $C_{12}E_8$ aggregates is ca. 90, meaning that the $C_{12}E_8$ micelles have about the same size in the absence and presence of PEG 12 kDa.

3. Isothermal Titration Microcalorimetry. The enthalpy of interaction between $C_{12}E_8$ and PEG was obtained by injecting a microvolume of a concentrated $C_{12}E_8$ (54 mM) or PEG (10 wt %) solution either in pure water or in PEG or $C_{12}E_8$ solution (Figures 12 and 13). The titration calorimetry measurements were made at 25 °C as a function of $C_{12}E_8$ (Figure 13a) or PEG (Figure 13b) concentration in the absence and presence of PEG 5.0 wt % or $C_{12}E_8$ 5.0 wt %.

(a) Binary $C_{12}E_8$/Water System. Figure 13a shows the observed enthalpy of $C_{12}E_8$ in water, around and above its cmc $\approx (7-9) \times 10^{-5}$ M (25 °C).[19] For the binary $C_{12}E_8$/water and ternary $C_{12}E_8$/PEG/water ΔH_{obs} is always exothermic. Around cmc a fraction of the added micelles breaks up to form unimers while the remaining surfactant is in the micellar form ($\Delta H_{obs} = \Delta H_{dil} + \Delta H_{demic}$). At higher $C_{12}E_8$ concentrations the micelles are simply diluted in water, and the enthalpy change is then due to intermicellar interactions ($\Delta H_{obs} = \Delta H_{dil}$).

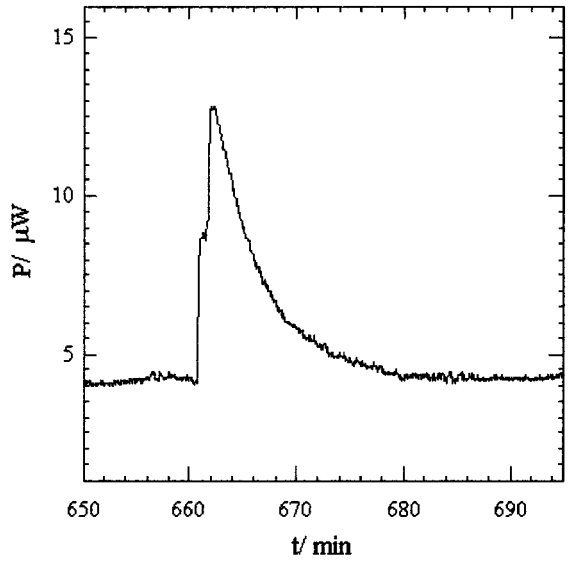

Figure 12. Typical thermal power for an injection during a titration experiment of 10 wt % $C_{12}E_8$ with 10 wt % PEG.

(b) Ternary PEG/$C_{12}E_8$/Water System. Figure 13a shows the titration curve for the addition of concentrated $C_{12}E_8$ micellar solution into a 5.0 wt % PEG solution. The difference between the titration curve in the polymer solution and in water is ascribed to the $C_{12}E_8$−PEG interaction (≈1 kJ mol^{-1}). Comparison of the curves for the PEG and PEG-free solutions (Figure 13a) reveals that in the presence of PEG the enthalpy of interaction becomes more exothermic. The cmc of $C_{12}E_8$ is about the same in both the presence and absence of PEG as reported for the interaction of other nonionic surfactants with neutral polymer.[9,11] PEG does not change the cmc of $C_{12}E_8$ (cmc ≈ cac) despite the affinity of PEG for $C_{12}E_8$, suggesting that the micellar aggregates rather than the monomers drive the PEG−$C_{12}E_8$ complexation and that the excluded volume is the driving force for complexation in such systems, as reported previously.[8−10]

When titrating $C_{12}E_8$ 5.0 wt % (in the vessel) with 10 wt % of PEG (in the syringe), an exothermic enthalpy of interaction was also obtained (Figure 13b). The experimental potential (thermopile voltage) vs time curve was deconvoluted (Figure 12) by adding to the original signal its time derivative multiplied by the time constant as described by the simple Tian equation, $P = \epsilon_c(V + \tau\, dV/dt)$, where P is the thermal power (in watts), τ is the time constant (in seconds) of the instrument, ϵ_c is a calibration constant, and dV/dt is the time derivative of the voltage signal. The corrected curve has a higher noise level since the time derivative of the potential signal is used to correct the voltage output. We can observe that each response consists of two exothermic peaks, suggesting that the mechanism of interaction between PEG and $C_{12}E_8$ micelles involves two steps, probably one associated with dilution of the micellar solution and the other the formation of the complexes. The enthalpies shown in Figure 13b are the sum of both peaks. The titration calorimetry results show the occurrence of an exothermic $C_{12}E_8$−PEG association, which yields, together with those from time-resolved fluorescence, that the slow mode observed in the relaxation time distributions does not reflect segregation (but complexation) of the components in the mixtures.

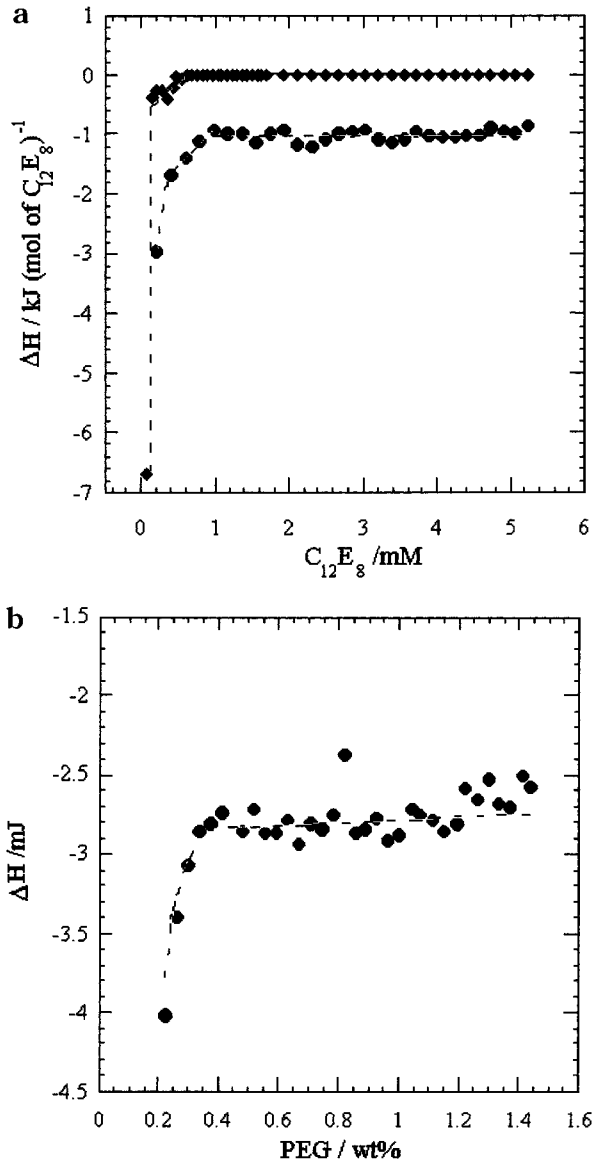

Figure 13. Observed enthalpy (a) for addition of a 54 mM $C_{12}E_8$ micellar dispersion into pure water (◆) and into PEG 5.0 wt % aqueous solution (●) and (b) of a 10 wt % PEG solution into $C_{12}E_8$ 10 wt % micellar solution (25 °C).

Conclusions

Mixing low molar mass PEG (M_w = 12 kDa) with the nonionic surfactant $C_{12}E_8$ yields PEG/$C_{12}E_8$ complexes whose structure and size depend on the amount of both surfactant and polymer. The enthalpy of interaction of $C_{12}E_8$ with PEG obtained with titration calorimetry is exothermic and equals 1 kJ mol^{-1}. According to our results of DLS and TRFQ, possible structures of the PEG/$C_{12}E_8$ complex consist of one or more $C_{12}E_8$ micelles surrounded by a PEG chain. At low concentrations of either the polymer or the surfactant (or both), the complex probably contains a single micelle within a polymer coil, whereas at higher concentrations of the components two or possibly three micelles are associated with the polymer giving rise to larger sized complexes. The fluorescence and calorimetry corroborate the scattering experiments and also suggest complex formation.

Since low molecular weight PEG is unusual in its solubility in both water and benzene, it would appear to be this characteristic which drives the perhaps unexpected interaction of PEG with the micelle/water interface. The present results do not contradict the findings of Anthony and Zana.[6] In their study, these authors used a very low concentration of surfactant (0.3 wt %) and different temperatures. While we would concur that at this surfactant level the aggregation number is essentially unchanged from that in the binary surfactant solutions, this does not mean an absence of interaction between the two components

Acknowledgment. E.F. thanks Conselho Nacional de Desenvolvimento Científico e Tecnológico (CNPq) for stipendium (Grant 201720/93-0), Fundação de Coordenação de Aperfeiçoamento de Pessoal de Nível Superior (CAPES), and Fundação de Amparo à Pesquisa do Estado de São Paulo (FAPESP) (Grant 98/09772-4) for partial support. P.C.A.B. acknowledges the PRAXIS XXI, JNICT for financial support, scholarship BD/13788/97.

References and Notes

(1) Lindman, B.; Thalberg, K. In *Interactions of Surfactants with Polymers and Proteins*; Goddard, E., Ananthapadmanabhan, K. P., Eds.; CRC Press: Boca Raton, FL, 1993; p 203.
(2) Hayakawa, K.; Kwak, J. C. In *Cationic Surfactants. Physical Chemistry*; Surfactant Science Series; Rubingh, D. N., Holland, P. M., Eds.; Marcel Dekker: New York, 1991; Vol. 37, p 189.
(3) Goddard, E. D. *Colloids Surf.* **1986**, *19*, 255, 301.
(4) Goddard, E. D. In *Interactions of Surfactants with Polymers and Proteins*; Goddard, E., Ananthapadmanabhan, K. P., Eds.; CRC Press: Boca Raton, FL, 1993; p 219.
(5) Breuer, M. M.; Robb, I. D. *Chem. Ind. (London)* **1972**, *13*, 530.
(6) Anthony, O.; Zana, R. *Langmuir* **1994**, *10*, 4048.
(7) Brackman, J. C.; Engberts, J. B. F. N. *Chem. Soc. Rev.* **1993**, *22*, 8.
(8) Feitosa, E.; Brown, W.; Hansson, P. *Macromolecules* **1996**, *29*, 2169.
(9) Feitosa, E.; Brown, W.; Vasilescu, M.; Swanson-Vethamuthu, M. *Macromolecules* **1996**, *29*, 6837.
(10) Feitosa, E.; Brown, W.; Swanson-Vethamuthu, M. *Langmuir* **1996**, *12*, 5985.
(11) Brackman, J. C.; van Os, N. M.; Engberts, J. B. F. N. *Langmuir* **1988**, *4*, 1266.
(12) Fundin, J.; Brown, W. *Macromolecules* **1994**, *27*, 5024.
(13) Winnik, F. M.; Regismond, S. T. A. *Colloids Surf. A* **1996**, *118*, 1.
(14) Jakes, J. *Czech. J. Phys.* **1988**, *B38*, 1305.
(15) Provencer, S. W. *Makromol. Chem.* **1979**, *180*, 201.
(16) Almgren, M.; Hansson, P.; Mukhtar, E.; van Stam, J. *Langmuir* **1992**, *8*, 2405.
(17) (a) Infelta, P. P.; Grätzel, M.; Thomas, J. K. *J. Phys. Chem.* **1974**, *78*, 190. (b) Infelta, P. P.; Grätzel, M. *J. Chem. Phys.* **1983**, *78*, 5280. (c) Tachiya, M. *Chem. Phys. Lett.* **1975**, *33*, 289. (d) Tachiya, M. *J. Chem. Phys.* **1982**, *76*, 340; **1983**, *78*, 5282.
(18) Briggner, L.-E.; Wadsö, I. *J. Biochem. Biophys. Methods* **1991**, *22*, 101.
(19) (a) Andersson, B.; Olofsson, G. *J. Chem. Soc., Faraday Trans. 1* **1988**, *84*, 4087. (b) Deguchi, K.; Meguro, K. *J. Colloid Interface Sci.* **1972**, *38*, 595.

MA010696W